Nuclear Physics B267 (1986) 509–530

HIGGS PRODUCTION AT e^+e^- COLLIDERS

A. BARROSO, J. PULIDO and J.C. ROMÃO

CFN/CFMC, Universidades de Lisboa, Gama Pinto 2, Lisboa, Portugal

Received 21 August 1985

We perform a complete one-loop calculation of the process $e^+e^- \to H\gamma$. The W-loop diagrams contributing to the $ZH\gamma$ and $\gamma H\gamma$ three-point functions contain divergencies. So, the calculation of this process requires a careful examination of the renormalization scheme. This we do and we also discuss in detail the gauge invariance of the various amplitudes. The results for the cross section are compared with those for the reaction $e^+e^- \to H\mu^+\mu^-$.

1. Introduction

A unified and beautiful description of the weak and electromagnetic interactions is given by the Glashow–Weinberg–Salam [1] (GWS) theory based on the gauge group $SU_L(2) \times U_Y(1)$. Several experimental successes have been credited to this model ranging from the evidence for weak neutral currents [2] in 1973 to the recent discovery of the gauge bosons [3], W and Z, at the CERN collider. However, it is fair to say that the fundamental mechanism [4] responsible for the gauge bosons masses remains untested, and the scalar sector of the theory is the least understood aspect of the GWS model. Yet, the dynamics of this sector has to account for the most interesting feature of the standard model, namely, the spontaneous breaking of the gauge symmetry.

As a remnant of this Higgs mechanism [4] there is a neutral scalar particle, the Higgs boson, whose mass, M_H, is constrained only to lie within the range 7 GeV$/c^2$ [5] to 1 TeV$/c^2$ [6]. While the lower bound can be avoided introducing more than one Higgs doublet, the upper bound is almost model independent. In fact, if M_H exceeds 1 TeV$/c^2$ one would have, at least, a strongly interacting Higgs sector, which, most likely, would be the signal of new physical phenomena. Leaving aside this possibility, it must be clear that the discovery of the Higgs particle is the only way of testing the corner-stone of the whole theory: the breaking of $SU(2) \times U(1)$ down to $U(1)$. Hence, experimental searches for H will be carried out at future electron-positron and hadron colliders.

Our purpose in this paper is to consider in detail the Higgs production via the reaction $e^+e^- \to H\gamma$. The tree-level amplitude for this process is extremely small because it is proportional to m_e^2/M_W^2. So, the dominant contribution to the cross section comes from one-loop diagrams. Those were studied previously by Leveille [7] but we will prove that his results are not correct. Contrary to his claims [7] the amplitude of the W triangle loop is not finite nor gauge invariant. So, its calculation requires that one specifies a renormalization scheme for the GWS theory. Once this is done and the appropriate counterterms are included the infinities cancel. This cancellation gives rise to finite contributions but for a Z boson off-shell the amplitude is still not gauge invariant. Obviously, the amplitude for $e^+e^- \to H\gamma$ must be gauge invariant. We will show that this is so because there are other Feynman diagrams, not considered before, that restore the gauge invariance.

We organize our paper in the following way. In sect. 2 we calculate the Green functions $ZH\gamma$ and the $\gamma H\gamma$ with the out-going particles (H, γ) on-shell and the incoming one (Z or γ) off-shell. We discuss in detail the contribution of the diagrams with W loops because in the GWS model to extract finite terms from loop diagrams it is not sufficient to throw away the divergent pieces. In sect. 3 we calculate the remaining diagrams that contribute to the reaction $e^+e^- \to H\gamma$ and show that the total amplitude is gauge invariant. In sect. 4 we present our results and discuss the possibility of using this reaction to detect the Higgs at future e^+e^- colliders. For comparison we also re-calculate [8] the cross section for $e^+e^- \to H\mu^+\mu^-$. At the peak of the Z resonance the Higgs production was investigated by other authors, who calculated the partial widths as $\Gamma(Z \to H\mu^+\mu^-)$ [9] and $\Gamma(Z \to H\gamma)$ [10]. Our results are in agreement with theirs.

2. The ZHγ and the γHγ three-point functions

In the standard model the $ZH\gamma$ coupling is not present at the tree level. Actually, one can go even further and show [11] that the same is true for any weak gauge model that after symmetry breaking contains the electromagnetic U(1) group. At one loop, the $ZH\gamma$, $T_Z^{\rho\mu}$, and $\gamma H\gamma$, $T_G^{\rho\mu}$, three-point functions contain contributions from a W-boson loop and from fermion loops. For a reason that will become clear later we denote the fermionic contribution by $G^{\rho\mu}$, i.e., we write

$$T_A^{\rho\mu} = G_A^{\rho\mu}(\mathrm{F}) + T_A^{\rho\mu}(\mathrm{W}), \qquad A = \mathrm{Z} \text{ or } \mathrm{G} \tag{2.1}$$

2.1. FERMION LOOPS

To be specific let us consider $G_Z^{\rho\mu}$. In fig. 1 we show the usual triangle diagram, where k and k' are the 4-momenta of the outgoing photon and Higgs boson respectively, and q is the 4-momentum of the incoming Z. For our purpose it is sufficient to consider that the Higgs and the photon are on-shell, i.e., $k'^2 = M_H^2$ and $k^2 = \varepsilon \cdot k = 0$ where ε_μ is the photon polarization.

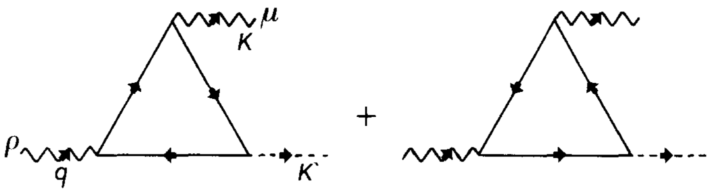

Fig. 1. Feynman diagrams corresponding to $G_A^{\rho\mu}(\mathrm{F})$.

The Z-fermion coupling is

$$\mathcal{L} = \frac{g}{\cos\theta_{\mathrm{W}}} Z_\mu J^\mu, \tag{2.2}$$

where the neutral current J^μ of fermion f is

$$J^\mu = \bar{\psi}_{\mathrm{f}}\left(g_{\mathrm{V}}^{\mathrm{f}}\gamma^\mu - g_{\mathrm{A}}^{\mathrm{f}}\gamma^\mu\gamma_5\right)\psi_{\mathrm{f}}, \tag{2.3}$$

with

$$g_{\mathrm{V}}^{\mathrm{f}} = \tfrac{1}{2}T_3^{\mathrm{f}} - Q_{\mathrm{f}}\sin^2\theta_{\mathrm{W}}, \tag{2.4a}$$

$$g_{\mathrm{A}}^{\mathrm{f}} = \tfrac{1}{2}T_3^{\mathrm{f}}. \tag{2.4b}$$

T_3^{f} and Q_{f} are the third component of the weak isospin and the fermion charge, in units of $e > 0$, respectively. With similar notation the photon coupling is

$$\mathcal{L} = -eQ_{\mathrm{f}}\bar{\psi}_{\mathrm{f}}\gamma^\mu\psi_{\mathrm{f}}A_\mu \tag{2.5}$$

and the same Feynman diagrams enable us to obtain $G_G^{\rho\mu}(\mathrm{F})$. Both calculations proceed along similar lines and our results are

$$G_A^{\rho\mu}(\mathrm{F}) = -\frac{eg}{4\pi^2 M_{\mathrm{W}}}\left[k\cdot q g^{\rho\mu} - k^\rho q^\mu\right]\sum_{\mathrm{f}} Q_{\mathrm{f}} C_A^{\mathrm{f}}\left[J_1(\beta', \beta'_{\mathrm{H}}) - 4J_2(\beta', \beta'_{\mathrm{H}})\right], \tag{2.6}$$

with

$$C_A^{\mathrm{f}} = \begin{cases} g g_{\mathrm{V}}^{\mathrm{f}}/\cos\theta_{\mathrm{W}}, & \text{if } A = \mathrm{Z} \\ -eQ_{\mathrm{f}}, & \text{if } A = \mathrm{G}. \end{cases} \tag{2.7}$$

J_1 and J_2 are dimensionless parametric integrals given in the appendix and $\beta' = q^2/m_{\mathrm{f}}^2$, $\beta'_{\mathrm{H}} = M_{\mathrm{H}}^2/m_{\mathrm{f}}^2$. The sum in eq. (2.6) runs over all fermions but, essentially, only the top quark, t, is relevant. For instance, with $q^2 = M_{\mathrm{Z}}^2$ and $m_{\mathrm{t}} = M_{\mathrm{H}} = 40$ GeV$/c^2$, the bottom and charm quarks give a contribution to $|G_{\mathrm{Z}}^{\rho\mu}|$ which is 3% and 0.5% of the top value, respectively.

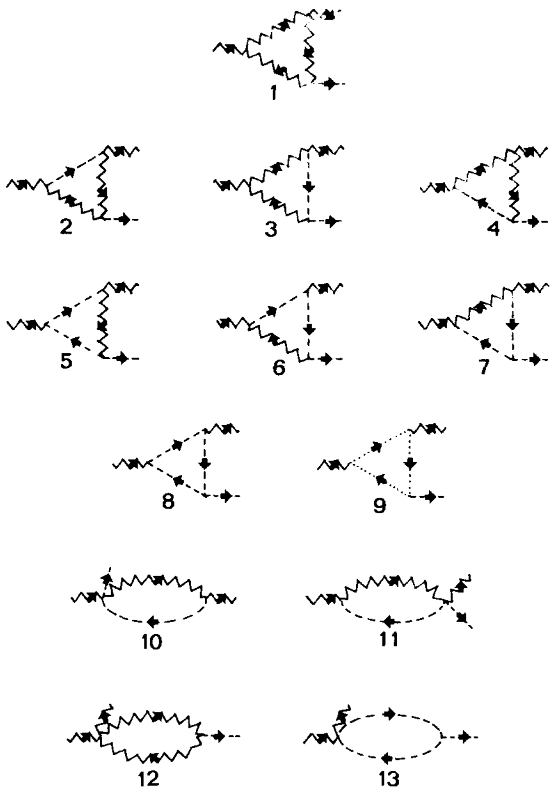

Fig. 2. W-loop diagrams corresponding to $T_A^{\rho\mu}(\mathrm{W})$.

Before we consider the W-loop diagrams there are two small comments that ought to be made. Firstly, notice that $G_A^{\rho\mu}$ is proportional to the square of the fermion mass, one power of m_f due to the Higgs coupling and the other one stemming from the trace over the γ-matrices. Secondly, let us remark that the triangles of fig. 1 are by themselves finite and gauge invariant, i.e., $k_\mu G_A^{\rho\mu}(\mathrm{F}) = 0$. We will see that this statement is not true for the W diagrams.

2.2. W-BOSON LOOPS

The physical content of the GWS theory is transparent in the unitary gauge. But, in this gauge, Green functions contain extra divergencies [12] that cannot be removed by renormalization counterterms. Hence, we work in the 't Hooft-Feynman (HF) gauge in which the vector propagators have the simplest form. The price one pays is the introduction of unphysical scalar fields.

In fig. 2 we show the relevant diagrams to the calculation of $T_A^{\rho\mu}(\mathrm{W})$ in the HF gauge. Notice that for each of diagrams 1 to 11 there is a crossed one which corresponds to a loop circulation in the opposite direction. These are not displayed in the figure but, when we refer to a particular diagram it should be understood that the crossed one is also included. The Feynman rules are either shown explicitly in ref. [13] or they can be trivially obtained from the lagrangian given there. We follow the work of Sakakibara [13] which exploits with some modifications the renormalization procedure of Ross and Taylor [14]. This is essentially an on-shell renormalization scheme where the parameters that characterize the theory are e, M_W, M_Z, M_H and m_f. Then the renormalized gauge couplings are such that $g\sin\theta_W = g'\cos\theta_W = e$ and the Weinberg angle θ_W is fixed by the gauge bosons masses, i.e., $\cos\theta_W = M_W/M_Z$.

The diagrams 8 and 13 are directly proportional to the Higgs mass and give the following gauge invariant contribution:

$$G_A^{\rho\mu}(8+13) = -\frac{eg}{8\pi^2 M_W}\left[k\cdot q g^{\rho\mu} - k^\rho q^\mu\right] C_A \left(\frac{M_H}{M_W}\right)^2 J_2(\beta,\beta_H), \tag{2.8}$$

with

$$C_A = \begin{cases} g\cos\theta_W\left(1-\tan^2\theta_W\right), & \text{if } A = Z \\ -2e, & \text{if } A = G \end{cases} \tag{2.9}$$

and $\beta = q^2/M_W^2$, $\beta_H = M_H^2/M_W^2$. The remaining diagrams of fig. 2 contain divergent pieces. We evaluate them using dimensional regularization. Since this is one of the main issues of this paper let us elaborate on this point. Using the Feynman parametrization for the propagators and integrating over the loop 4-momentum in dimension $d = 4-\varepsilon$ one obtains

$$T_Z^{\rho\mu}(1,\ldots,7,9,\ldots,12) = \frac{eg^2\cos\theta_W M_W}{16\pi^2}\left\{-\tfrac{1}{2}\int_0^1 dx_1 \int_0^{1-x_1} dx_2 \times \Delta^{-\varepsilon/2}\Gamma\left(\tfrac{1}{2}\varepsilon\right)\left(\alpha+\beta\tan^2\theta_W\right)g^{\rho\mu} + \text{finite terms}\right\}, \tag{2.10}$$

with

$$\Delta = M_W^2\left[1 - \beta x_1(1-x_1) + (\beta-\beta_H)x_1x_2\right].$$

The divergent parts are explicitly shown as poles of the gamma function, Γ, when $\varepsilon \to 0$ and the values of α and β are displayed in table 1. The corresponding result for the $\gamma H\gamma$ three-point function can be obtained from eq. (2.10) with the substitutions $g\cos\theta_W \to -e$ and $\tan^2\theta_W \to -1$. Bearing in mind that the total values of α and β are equal it is clear that in $T_G^{\rho\mu}$ the divergencies cancel exactly. On the

TABLE 1
Values of α and β for eq. (2.10)

Diagram	α	β
1	$12(3-\varepsilon)$	0
2	0	0
3	$-3+\varepsilon$	0
4	0	$3-\varepsilon$
5	1	-1
6	0	-2
7	0	0
9	-2	0
10	0	$4-\varepsilon$
11	0	$4-\varepsilon$
12	$-8(3-\varepsilon)$	0
Total	$8-3\varepsilon$	$8-3\varepsilon$

contrary, they do not cancel in $T_Z^{\rho\mu}$ which means that there must be an appropriate counterterm in the GWS lagrangian. To see how it arises consider the following part of the lagrangian,

$$\mathcal{L}_H = \tfrac{1}{4}\varphi v\left[g^2 A_{3\mu}A^{3\mu} + g'^2 B_\mu B^\mu + 2gg' A_{3\mu}B^\mu\right], \tag{2.11}$$

where B_μ and $A_{3\mu}$ are the gauge fields corresponding to $U_Y(1)$ and the third component of SU(2), respectively; φ denotes the Higgs field and v is the vacuum expectation value. To generate the counterterms one uses the transformations [13]:

$$\begin{aligned} A_{3\mu} &\to Z_W^{1/2} A_{3\mu}, \qquad g \to Z_W^{-1/2}(g+\delta g), \\ B_\mu &\to Z_B^{1/2} B_\mu, \qquad g' \to Z_B^{-1/2}(g'+\delta g'), \\ \varphi &\to Z_\varphi^{1/2}\varphi, \qquad v \to Z_\varphi^{1/2}(v+\delta v). \end{aligned} \tag{2.12}$$

Then, writing $Z_i = 1+\delta Z_i$ and recalling that the renormalized fields satisfy the equations

$$\begin{aligned} A_3^\mu &= Z^\mu \cos\theta_W - A^\mu \sin\theta_W, \\ B^\mu &= Z^\mu \sin\theta_W + A^\mu \cos\theta_W, \end{aligned} \tag{2.13}$$

one obtains

$$\mathcal{L}_H = \frac{g}{2\cos\theta_W} M_Z Z_\mu Z^\mu \varphi + \mathcal{L}^c, \tag{2.14a}$$

with

$$\mathcal{L}^{c} = M_Z Z_\mu Z^\mu \varphi(\cos\theta_W \delta g + \sin\theta_W \delta g')$$
$$+ M_W Z_\mu A^\mu \varphi(\delta g' - \tan\theta_W \delta g)$$
$$+ \frac{g}{2\cos\theta_W} M_Z Z_\mu Z^\mu \varphi(\delta Z_\varphi + \delta v). \tag{2.14b}$$

The first term of eq. (2.14a) leads to the normal ZZH coupling while the second term of eq. (2.14b) is the ZHγ counterterm.

Evaluating $\delta g'$ and δg at one-loop level the results are [13]

$$\delta g' = 0, \tag{2.15a}$$

$$\delta g = -\frac{g^3}{8\pi^2}\Gamma(\tfrac{1}{2}\varepsilon)(M_W^2)^{-\varepsilon/2}. \tag{2.15b}$$

Inserting these equations into $\mathcal{L}^c$ we obtain

$$T_Z^{\rho\mu}(\text{counterterm}) = \frac{eg^2\cos\theta_W M_W}{16\pi^2}(1+\tan^2\theta_W)$$
$$\times g^{\rho\mu} 2\Gamma(\tfrac{1}{2}\varepsilon)(M_W^2)^{-\varepsilon/2}. \tag{2.16}$$

Adding this contribution to the sum $\Sigma_i T_Z^{\rho\mu}(i)$, with $i = 1,\dots,7,9,\dots,12$, it is easy to see that the divergencies cancel and, in the $\varepsilon \to 0$ limit, a finite term survives, i.e.,

$$\lim_{\varepsilon\to 0}\left\{2\Gamma(\tfrac{1}{2}\varepsilon)(M_W^2)^{-\varepsilon/2} - \tfrac{1}{2}(8-3\varepsilon)\Gamma(\tfrac{1}{2}\varepsilon)\int_0^1 \mathrm{d}x_1 \int_0^{1-x_1}\mathrm{d}x_2 \Delta^{-\varepsilon/2}\right\}$$
$$= 4\int_0^1 \mathrm{d}x_1 \int_0^{1-x_1}\mathrm{d}x_2 \ln\frac{\Delta}{M_W^2}. \tag{2.17}$$

Perhaps, it is instructive to use an alternative approach* to prove the finiteness of $T_Z^{\rho\mu}(\mathrm{W})$. Due to loop corrections there is a Zγ mixing. Inserting the Higgs field in all one-loop Zγ mixing diagrams one obtains the Feynman graphs of fig. 2 plus the extra reducible diagrams shown in fig. 3. The evaluation of these diagrams, for an outgoing photon on-shell, is straightforward. Diagrams 1 and 2 vanish, as they should, since there is no need for a fermion counterterm. In fact, one can be more precise and show [13] that the fermion contribution to the Zγ mixing is proportional

* In our renormalization scheme there is no physical condition to be imposed on the Zγ mixing. So, in principle, the results obtained in the second approach could have an undefined finite part.

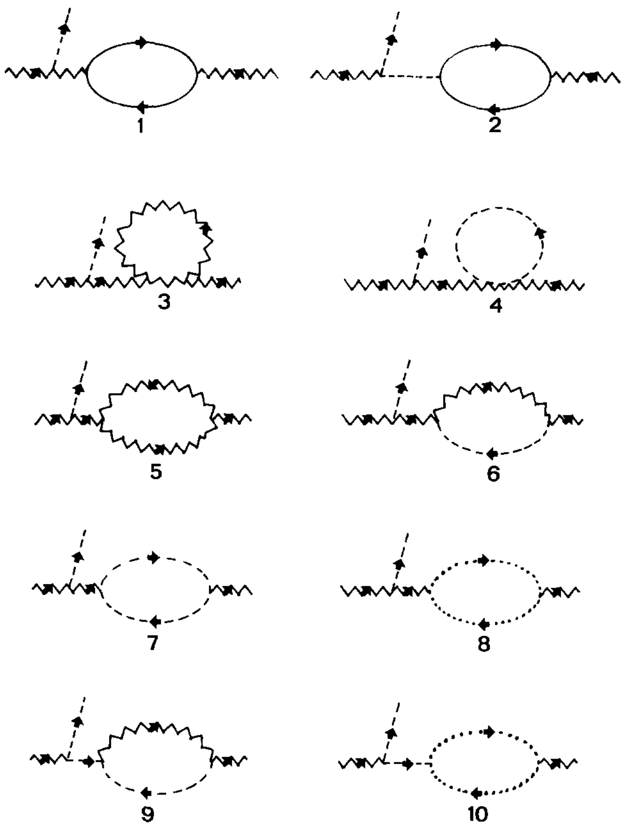

Fig. 3. Reducible diagrams for ZHγ.

to k^2. The same is true for diagrams 9 and 10 but, all the others contain divergencies that can be written in the general form

$$T_Z^{\rho\mu}(3,\dots,8) = \frac{eg^2 \cos\theta_W M_W}{16\pi^2} g^{\rho\mu}\left(M_W^2\right)^{-\varepsilon/2}\left(\alpha + \beta \tan^2\theta_W\right). \qquad (2.18)$$

The values of α and β are shown in table 2, and looking at this table it is immediately seen that the sum of these graphs reproduces eq. (2.16).

Although the calculation of $T_A^{\rho\mu}(\mathrm{W})$ is lengthy there are no further points that deserve to be mentioned. Including the result of eq. (2.8) our final answer is

$$T_A^{\rho\mu}(\mathrm{W}) = G_A^{\rho\mu}(\mathrm{W}) + X_A^{\rho\mu}, \qquad (2.19)$$

TABLE 2
Values of α and β for eq. (2.18)

Diagram	α	β
3	$2(3-\varepsilon)\Gamma(-1+\frac{1}{2}\varepsilon)$	0
4	$\Gamma(-1+\frac{1}{2}\varepsilon)$	$-\Gamma(-1+\frac{1}{2}\varepsilon)$
5	$-3(3-\varepsilon)\Gamma(-1+\frac{1}{2}\varepsilon)$	0
6	0	$2\Gamma(\frac{1}{2}\varepsilon)$
7	$-\Gamma(-1+\frac{1}{2}\varepsilon)$	$\Gamma(-1+\frac{1}{2}\varepsilon)$
8	$\Gamma(-1+\frac{1}{2}\varepsilon)$	0
Total	$2\Gamma(\frac{1}{2}\varepsilon)$	$2\Gamma(\frac{1}{2}\varepsilon)$

with

$$G_A^{\rho\mu}(\mathrm{W}) = \frac{eg}{4\pi^2 M_\mathrm{W}}\left[k\cdot q g^{\rho\mu} - k^\rho q^\mu\right]\left[C_A J_1(\beta,\beta_\mathrm{H}) + D_A J_2(\beta,\beta_\mathrm{H})\right], \tag{2.20}$$

$$C_A = \begin{cases} g\cos\theta_\mathrm{W}\left(3-\tan^2\theta_\mathrm{W}\right), & \text{if } A=\mathrm{Z} \\ -4e, & \text{if } A=\mathrm{G}, \end{cases} \tag{2.21}$$

$$D_A = \begin{cases} g\cos\theta_\mathrm{W}\left[-5+\tan^2\theta_\mathrm{W} - \frac{1}{2}\beta_\mathrm{H}\left(1-\tan^2\theta_\mathrm{W}\right)\right], & \text{if } A=\mathrm{Z} \\ e(6+\beta_\mathrm{H}), & \text{if } A=\mathrm{G} \end{cases} \tag{2.22}$$

and

$$X_\mathrm{Z}^{\rho\mu} = -\frac{eg^2\cos\theta_\mathrm{W}}{16\pi^2 M_\mathrm{W}}\frac{1}{\beta-\beta_\mathrm{H}} \times\left\{\left[\tfrac{1}{2}\left(1+\tan^2\theta_\mathrm{W}\right)\Delta L + \left(2-\tan^2\theta_\mathrm{W}\right)\Delta S\right]q^\rho q^\mu - 3\left(q^2-M_\mathrm{Z}^2\right)\Delta S g^{\rho\mu}\right\}, \tag{2.23}$$

$$X_\mathrm{G}^{\rho\mu} = \frac{3e^2 g}{16\pi^2 M_\mathrm{W}}\frac{1}{\beta-\beta_\mathrm{H}}\Delta S\left[q^\rho q^\mu - q^2 g^{\rho\mu}\right]. \tag{2.24}$$

In the equations above, $L(x)$ and $S(x)$ are complex functions of the real variable x which are given in a previous paper [15] and we use the simplified notation $\Delta F = F(\beta) - F(\beta_\mathrm{H})$.

2.3. THE PARTIAL WIDTH FOR $Z \to H\gamma$

From our previous results it should be clear that $T_A^{\rho\mu}$ contains a piece, $X_A^{\rho\mu}$, which is not gauge invariant, i.e., $k_\mu X_A^{\rho\mu} \neq 0$. Nevertheless, for a real Z-boson with polarization 4-vector e_ρ we have

$$e_\rho X_Z^{\rho\mu}(q^2 = M_Z^2) = 0 .$$

Hence, the partial width for the decay $Z \to H\gamma$ depends only on $G_Z^{\rho\mu}$ and, a straightforward calculation leads to the result

$$\Gamma(Z \to H\gamma) = \frac{\sqrt{2}\,\alpha^2 G_F}{3\pi^3 \tan^2\theta_W} \left(\frac{M_Z^2 - M_H^2}{2M_Z} \right)^3 |I_{\Delta Z}|^2 , \tag{2.25}$$

with

$$I_{\Delta Z} = -\sum_f Q_f g_V^f (1 + \tan^2\theta_W) [J_1(\beta', \beta'_H) - 4J_2(\beta', \beta'_H)] + \frac{1}{g\cos\theta_W} [C_Z J_1(\beta, \beta_H) + D_Z J_2(\beta, \beta_H)] . \tag{2.26}$$

For later use it is convenient to define a similar quantity for the photon amplitude, namely:

$$I_{\Delta G} = \sum_f Q_f^2 [J_1(\beta', \beta'_H) - 4J_2(\beta', \beta'_H)] + \frac{1}{e} [C_G J_1(\beta, \beta_H) + D_G J_2(\beta, \beta_H)] . \tag{2.27}$$

Our eqs. (2.25) and (2.26) agree with the expression for the width $Z \to H\gamma$ derived by Cahn et al. [10]. On the other hand, let us stress, that in the $e^+e^- \to H\gamma$ amplitude, $\mathcal{M}$, there will be contributions from the non-gauge invariant terms $X_Z^{\rho\mu}$ and $X_G^{\rho\mu}$. Actually, we show in the next paragraph that the existence of such pieces is crucial to render $\mathcal{M}$ gauge invariant.

3. Cross section

Let us denote by $p_+(p_-)$ the momentum of the positron (electron) and by k the momentum of the photon. The differential cross section for detecting the photon making an angle θ with the direction of the incoming electron in the center of mass system is

$$\frac{d\sigma}{d(\cos\theta)} = \frac{1}{64\pi s} \frac{s - M_H^2}{2s} \sum_{\text{spins}} \left| \mathcal{M}\left(\theta, \omega = \frac{s - M_H^2}{2\sqrt{s}}\right) \right|^2 , \tag{3.1}$$

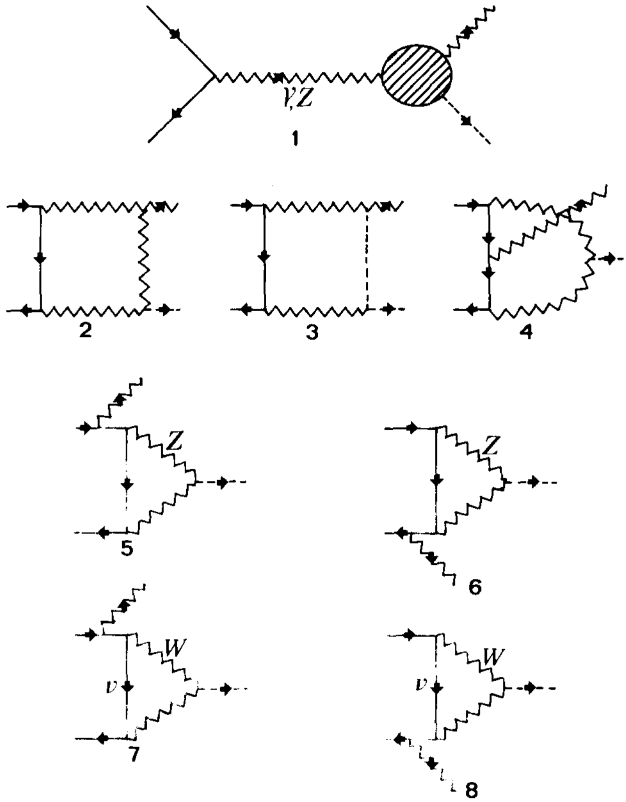

Fig. 4. Diagrams corresponding to the $e^+e^- \to H\gamma$ amplitude.

where $\sqrt{s}$ is the center of mass energy, ω the energy of the photon and $\mathcal{M}$ is the invariant T-matrix, i.e.,

$$\mathcal{M} = \varepsilon_\mu T^\mu . \tag{3.2}$$

In eq. (3.2) $\varepsilon^\mu(k)$ is the photon polarization vector and T^μ is the sum of the amplitudes of the diagrams in fig. 4 plus the tree-level amplitude T_0^μ. The last one is:

$$T_0^\mu = \tfrac{1}{2} eg \frac{m_e}{M_W} \bar{v}(p_+) \left[\frac{\not{k}\gamma^\mu - 2p_-^\mu}{2p_- \cdot k} - \frac{\gamma^\mu \not{k} - 2p_+^\mu}{2p_+ \cdot k} \right] u(p_-) . \tag{3.3}$$

Notice the factor m_e/M_W which gives a tremendous supression in the cross section. Furthermore, due to the spin trace the tree-level one-loop interference is also proportional to $(m_e/M_W)^2$. In the one-loop amplitudes we work in the $m_e = 0$ limit which means that we neglect the diagrams where the Higgs couples to the electron.

Using the results of sect. 2 we obtain

$$T_1^\mu = \frac{eg^3}{16\pi^2 M_W^3}\left[k\cdot q g^{\rho\mu} - k^\rho q^\mu\right]$$

$$\times\left[\bar{v}(p_+)\gamma_\rho u(p_-) 4\sin^2\theta_W \frac{M_W^2}{q^2} I_{\Delta G} + \bar{v}(p_+)\gamma_\rho(g_V^e - g_A^e\gamma_5)\right.$$

$$\left.\times u(p_-) 4\frac{M_W^2}{q^2 - M_Z^2} I_{\Delta Z}\right] + X_1^\mu, \tag{3.4}$$

with

$$X_1^\mu = e\bar{v}(p_+)\gamma_\rho u(p_-)\frac{1}{q^2}X_G^{\rho\mu}$$

$$+\frac{g}{\cos\theta_W}\bar{v}(p_+)\gamma_\rho(g_V^e - g_A^e\gamma_5)u(p_-)\frac{1}{q^2 - M_Z^2}X_Z^{\rho\mu}$$

$$= \tfrac{3}{2}eg^3 M_W \bar{v}\gamma_\rho \frac{1-\gamma_5}{2} u g^{\rho\mu}\frac{1}{16\pi^2}J_1(\beta, \beta_H). \tag{3.5}$$

Consistently with the $m_e = 0$ approximation we neglect the terms in $q^\rho q^\mu$.

Consider now the diagrams with a W-loop, namely, graphs 2 and 3 plus their crossing terms and diagrams 7 and 8. The result is

$$i(T_2^\mu + T_3^\mu + T_7^\mu + T_8^\mu) = \tfrac{1}{2}eg^3 M_W \int \frac{d^4p}{(2\pi)^4}\bar{v}(p_+)$$

$$\times\left\{\frac{A^\mu}{(p^2 - M_W^2)\left((p-q)^2 - M_W^2\right)\left((p-k)^2 - M_W^2\right)}\right.$$

$$+\frac{B^\mu}{(p^2 - M_W^2)\left((p+k-q)^2 - M_W^2\right)(p-p_+)^2}$$

$$\left.+\frac{C^\mu}{(p^2 - M_W^2)\left((p-k+q)^2 - M_W^2\right)(p+p_-)^2}\right\}$$

$$\times\frac{1-\gamma_5}{2}u(p_-), \tag{3.6}$$

with

$$A^\mu = 3\gamma^\mu - (p-p_+)^{-2}\big(-4\not{p}p^\mu + 4k\cdot(p-p_+)\gamma^\mu - 4(p-p_+)^\mu\not{k} + 2\not{p}[\gamma^\mu,\not{k}]\big)$$

$$-(p-p_-)^{-2}\big(-4\not{p}p^\mu + 4k\cdot(p-p_-)\gamma^\mu - 4(p-p_-)^\mu\not{k} + 2[\not{k},\gamma^\mu]\not{p}\big), \quad (3.7a)$$

$$B^\mu = \not{p}(\not{p}_- - \not{k})\gamma^\mu/p_-\cdot k, \quad (3.7b)$$

$$C^\mu = \gamma^\mu(-\not{p}_+ + \not{k})\not{p}/p_+\cdot k. \quad (3.7b)$$

Noting that

$$k\cdot A = 3\not{k} + 4p\cdot k\not{p}\big[(p-p_-)^{-2} + (p+p_+)^{-2}\big], \quad (3.8a)$$

$$k\cdot B = -k\cdot C = \not{p}, \quad (3.8b)$$

it is easy to show that

$$ik_\mu(T_1^\mu + T_2^\mu + T_3^\mu + T_7^\mu + T_8^\mu)$$

$$= eg^3 M_W \int \frac{d^4p}{(2\pi)^4}\bar{v}(p_+)\big[2p\cdot k - p^2 + M_W^2\big]\not{p}\frac{1-\gamma_5}{2}u(p_-)$$

$$\times (p^2 - M_W^2)^{-1}\big((p-q)^2 - M_W^2\big)^{-1}\big((p-k)^2 - M_W^2\big)^{-1}$$

$$\times\big[(p-p_+)^{-2} + (p-p_-)^{-2}\big]. \quad (3.9)$$

Note that the first term of eq. (3.8a) cancel the X_1^μ of eq. (3.4). It is also important to realize that we have made a change of variable $p \to -p+q$ and $p \to p-q$ in the B and C terms, respectively and at the same time we have multiplied the numerator and the denominator by $p^2 - M_W^2$. Now, the square bracket between the spinors of eq. (3.9) cancels with $(p-k)^2 - M_W^2$ and another change of variable, $p \to -p+q$, in the second integral of eq. (3.9) finally shows that it vanishes, i.e.

$$k_\mu \sum_i T_i^\mu = 0, \qquad i = 1,2,3,7,8. \quad (3.10)$$

Similarly, for diagrams 4–6, which have a Z loop, we obtain

$$i \sum_{i=4,5,6} T_i^\mu = \frac{eg^3 M_Z}{\cos\theta_W} \int \frac{d^4 p}{(2\pi)^4} \bar{v}(p_+)$$

$$\times \left\{ - \frac{2\not{p}\gamma^\mu(\not{p}-\not{k})}{p^2(p-k)^2\left((p-k+p_+)^2 - M_Z^2\right)\left((p-p_-)^2 - M_Z^2\right)} \right.$$

$$+ \frac{B^\mu}{(p^2 - M_Z^2)\left((p+k-q)^2 - M_Z^2\right)(p-p_+)^2}$$

$$\left. + \frac{C^\mu}{(p^2 - M_Z^2)\left((p-k+q)^2 - M_Z^2\right)(p+p_-)^2} \right\}$$

$$\times (g_V^e - g_A^e \gamma_5) u(p_-). \tag{3.11}$$

Again, a judicious change of the integration variable plus the use of the relation

$$\not{p}\not{k}\not{p} = -(\not{k}-\not{p})p^2 - \not{p}(p-k)^2,$$

enables one to show that

$$k_\mu \sum_{i=4,5,6} T_i^\mu = 0. \tag{3.12}$$

This completes the proof of the gauge invariance of the $e^+e^- \to H\gamma$ amplitude. We have done it with great detail because in the literature it is stated [7] incorrectly that the diagram 1 of fig. 4 is gauge invariant. However, for future reference, it is better if we summarize our results. In fact, each amplitude T_i may be written

$$T_i^\mu = \frac{eg^3}{16\pi^2 M_W^3} \bar{v}(p_+)\gamma_\rho(a_i - b_i\gamma_5)u(p_-)$$

$$\times \left\{ \left[k\cdot p_+ g^{\rho\mu} - k^\rho p_+^\mu\right] G_i^+ + \left[k\cdot p_- g^{\rho\mu} - k^\rho p_-^\mu\right] G_i^- \right\} + X_i^\mu, \tag{3.13}$$

where the expressions for $G_i^\pm$ and X_i and the values of a_i and b_i are given in table 3. Examining this table it becomes clear how the gauge invariance is accomplished.

There is one last point that it is worth a few comments. Although there is no tree level $H\gamma$ or HZ couplings one could naively expect that they would be generated via the diagrams of fig. 5b. If that was the case one would have an additional amplitude stemming from the Feynman graphs in fig. 5a. However, it is sufficient to recall the

TABLE 3
Values of the parameters of eq. (3.13)

Diagram	a_i	b_i	G_i^+	G_i^-	X_i^μ
1(G)	$4\sin^2\theta_W$	0	$\frac{M_W^2}{q^2} I_{\Delta G}$	$\frac{M_W^2}{q^2} I_{\Delta G}$	
1(Z)	$4g_V$	$4g_A$	$\frac{M_W^2}{q^2-\left(M_Z-\frac{1}{2}i\Gamma_Z\right)^2} I_{\Delta Z}$	$\frac{M_W^2}{q^2-\left(M_Z-\frac{1}{2}i\Gamma_Z\right)^2} I_{\Delta Z}$	X_1^μ
2 + 3	$\frac{1}{4}$	$\frac{1}{4}$	I_W^+	I_W^-	$-X_1^\mu - X_7^\mu - X_8^\mu$
4	$g_V^2 + g_A^2$	$-2g_A g_V$	I_Z^+	I_Z^-	$-X_5^\mu - X_6^\mu$
5	0	0	0	0	X_5^μ
6	0	0	0	0	X_6^μ
7	0	0	0	0	X_7^μ
8	0	0	0	0	X_8^μ

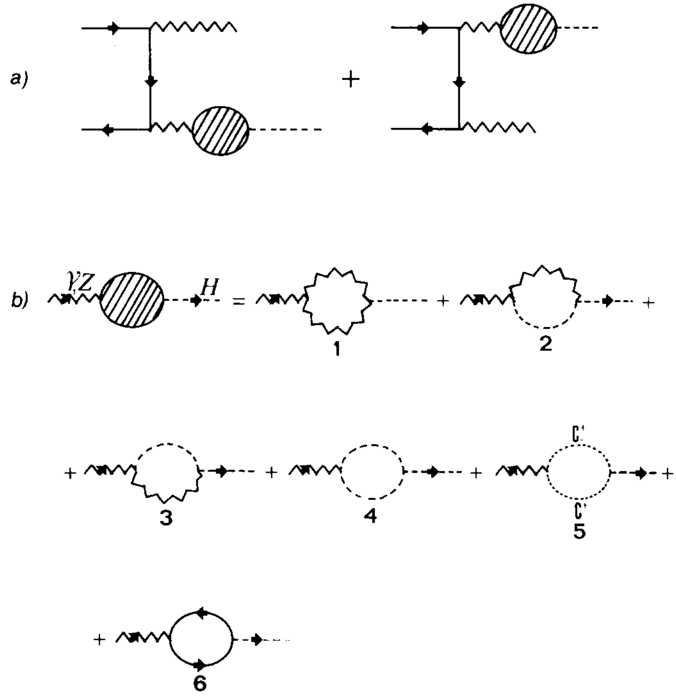

Fig. 5. (b) One-loop Z(γ)H mixing which is proved to vanish. Hence diagrams (a) do not exist.

CP invariance of the theory to show that such couplings cannot occur. A trivial calculation of the diagrams in fig. 5b confirms this result. Diagram 5 is zero when summed over both ghosts, diagrams 2 and 3 cancel each other and 1, 4 and 6 are proportional to the integral

$$I^{\alpha}=\int\frac{\mathrm{d}^d p}{(2\pi)^d}\frac{(2p-k)^{\alpha}}{(p^2-M^2)\left((p-k)^2-M^2\right)}\,.$$

A change of variable, $p \to -p+k$, proves that $I^{\alpha}=0$.

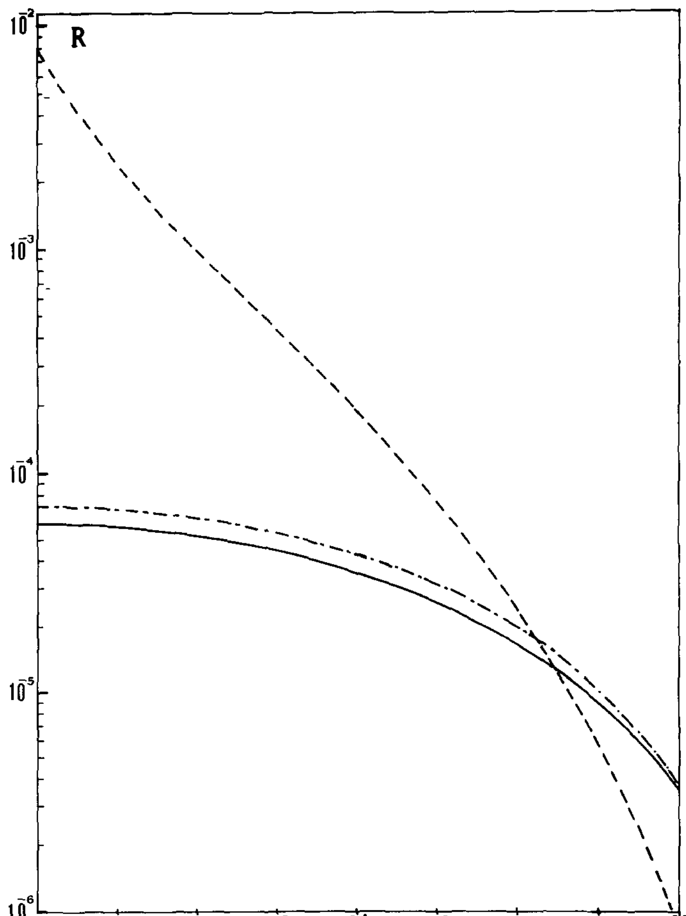

Fig. 6. The dashed curve is $\Gamma(Z\to H\mu^+\mu^-)/\Gamma(Z\to\mu^+\mu^-)$ and the full curve is $\Gamma(Z\to H\gamma)/\Gamma(Z\to\mu^+\mu^-)$. The dashed-dotted curve represents the second ratio evaluated only with the W contribution.

4. Results and discussion

In fig. 6 the dashed curve represents the ratio $R = \Gamma(Z \to H\mu^+\mu^-)/\Gamma(Z \to \mu^+\mu^-)$ as a function of M_H/M_Z. The Higgs production by this mechanism was considered previously [9] and for comparison we have repeated the calculation. In the same fig. the dashed-dotted curve represents the W-loop contribution to the ratio $R = \Gamma(Z \to H\gamma)/\Gamma(Z \to \mu^+\mu^-)$. Essentially, it reproduces the results of Cahn et al. [10]. The full curve is our result for the same relative width, R, including the fermionic contributions with a top quark with $m_t = 40$ GeV$/c^2$. We used $M_W = 80.8$ GeV$/c^2$ and $\sin^2\theta_W = 0.21$. It is clear that the fermion loops reduce $\Gamma(Z \to H\gamma)$. This, in turn, implies a slight shrinkage of the region of Higgs masses where the $H\gamma$ channel competes favourably with $H\mu^+\mu^-$. From this point of view it is good that the fermion triangle gives a rather small result, in comparison with the one obtained from the W diagrams. Roughly speaking, the reason for this is twofold. On one hand, the Higgs coupling is larger for particles with large mass. On the other hand, the C-parity of the photon and the Higgs implies that the Z couples to the triangle only through the vector coupling g_V^f which for up quarks is supressed relative to g_A^f by almost a factor of three.

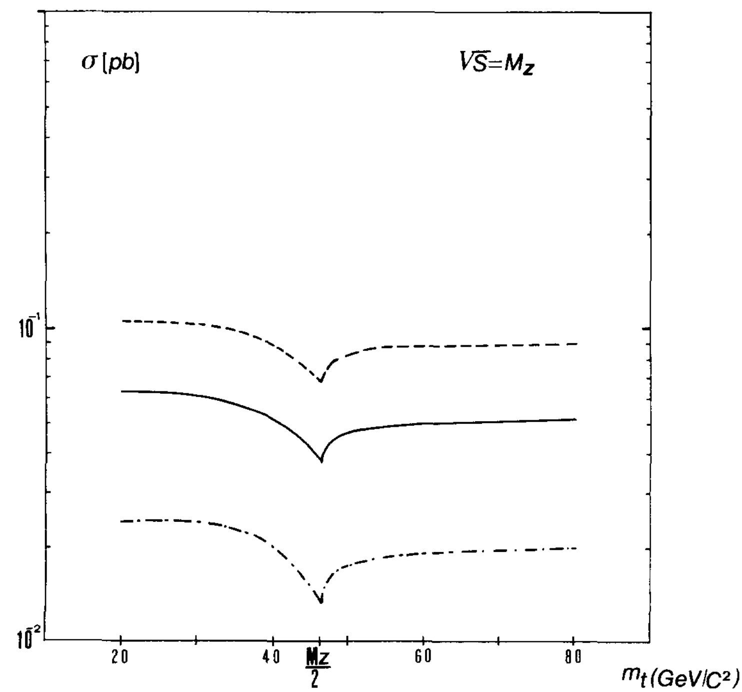

Fig. 7. σ as a function of the top quark mass, for three values of the Higgs mass: $---M_H = 10$ GeV, $—M_H = 40$ GeV and $\cdot\cdot\cdot M_H = 60$ GeV.

TABLE 4

Values of $\sigma(e^+e^- \to H\gamma)$ in pbarn. Each column gives a partial contribution to σ

$\sqrt{s}$	$\lvert T_0\rvert^2$	Interference T_0 triangle	$\lvert T_Z\rvert^2$	$\lvert T_G\rvert^2$	Interference T_Z, T_G	$\lvert T_{box}\rvert^2$	Interference box, triangle
60	8.1×10^{-8}	5.1×10^{-11}	6.9×10^{-6}	1.2×10^{-5}	-1.4×10^{-6}	2.7×10^{-7}	-2.9×10^{-7}
80	3.1×10^{-8}	4.2×10^{-12}	2.1×10^{-4}	3.8×10^{-6}	-4.4×10^{-6}	2.2×10^{-6}	3.1×10^{-5}
M_Z	2.1×10^{-8}	1.6×10^{-11}	5.1×10^{-2}	6.2×10^{-5}	1.1×10^{-4}	5.5×10^{-6}	9.7×10^{-5}
100	1.7×10^{-8}	1.4×10^{-10}	3.3×10^{-3}	8.7×10^{-5}	8.3×10^{-5}	8.4×10^{-6}	-2.9×10^{-4}
120	1.2×10^{-8}	9.6×10^{-11}	6.1×10^{-4}	1.5×10^{-4}	4.7×10^{-5}	2.5×10^{-5}	-2.8×10^{-4}
150	7.2×10^{-9}	8.8×10^{-11}	5.3×10^{-4}	3.1×10^{-4}	6.4×10^{-5}	1.4×10^{-4}	-7.4×10^{-4}

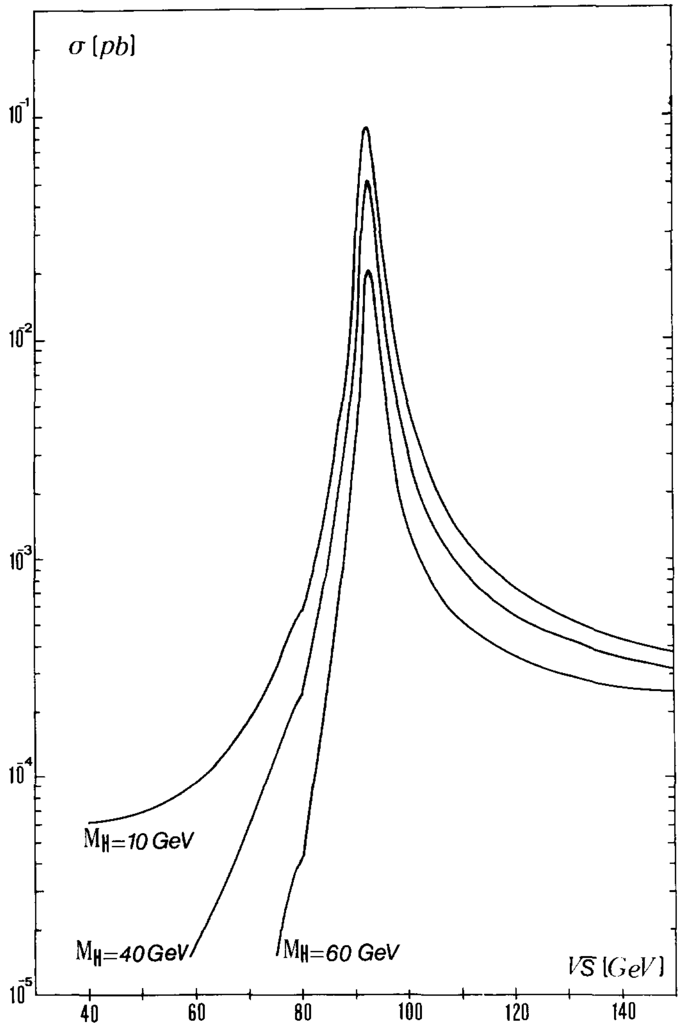

Fig. 8. Total $e^+e^- \to H\gamma$ cross section.

The sensitivity to the top mass can be seen in fig. 7 where we plot the $e^+e^- \to H\gamma$ total cross section, σ, for $\sqrt{s} = M_Z$ as a function of m_t. For small values of m_t ($m_t \lesssim 20$ GeV/c^2) we have essentially the result due to the W graphs, σ(W). Notice that the result of each fermion decreases with m_f^2/s when m_f goes to zero. When m_t becomes very large ($m_t \gtrsim 80$ GeV/c^2) σ tends asymptotically to a value, roughly 80% of σ(W), which corresponds to the limit $m_t \to \infty$. At $\frac{1}{2}M_Z$, and in general when $\sqrt{s} = 2m_t$, there is a deep in the cross section corresponding to the largest contribution of the top quark. This is a well-known threshold effect.

At the peak of the Z resonance it is a very good approximation to use the width $\Gamma(Z \to H\gamma)$ to estimate the number of $H\gamma$ events. This is illustrated in table 4 where, for several values of $\sqrt{s}$ and for $M_H = m_t = 40$ GeV/c^2 we present the partial contributions to σ. Notice that, at $\sqrt{s} = M_Z$, the resonance diagram is greater than the largest of the other terms by a factor of 500! It is also interesting to point out that the tree level amplitude is always negligible. In the most favourable case (small value of $\sqrt{s}$), it is smaller than the dominant term by more than two orders of magnitude.

A plot of σ as a function of $\sqrt{s}$ is shown in fig. 8. As expected, the cross section rises sharply when $\sqrt{s}$ approaches M_Z, but it is always smaller than 0.1 pbarn. So, a few GeV away from the peak σ becomes too small for the reaction to be seen. Using the value of the expected LEP luminosity we estimate that σ must be larger than 8×10^{-3} pb to have one event per month of running time. Despite the fact that the $e^+e^- \to H\gamma$ reaction has a very clean signature, we believe that a rate of one event per month must be close to the limit of experimental feasibility. Accepting this we conclude that the $H\gamma$ mode offers a good chance of detecting the Higgs boson if $M_H \lesssim 80$ GeV/c^2. Unfortunately, if $M_H > 80$ GeV/c^2 the alternative channel, $H\mu^+\mu^-$, is not better. Its cross section is larger and rises slightly with energy but, even at LEP II energies ($\sqrt{s} = 150$ GeV) it is 3.7×10^{-4}, 4.9×10^{-5} and 3.5×10^{-6} pb for $M_H = 80$, 100 and 120 GeV/c^2 respectively.

Appendix

MOMENTUM INTEGRATION

After using the Feynman parametrization the momentum integration can be performed using the general formula

$$\int \frac{d^d p}{(2\pi)^d} \frac{p_{\mu 1} p_{\mu 2} \cdots p_{\mu N}}{\left(p^2 + 2p\cdot P - M^2 + i\varepsilon\right)^n}$$

$$= \frac{(-1)^n i\pi^{d/2}}{(2\pi)^d \Gamma(n)} \int_0^\infty \frac{dt}{(2t)^N} t^{n-1-d/2} \frac{\partial}{\partial P^{\mu 1}} \cdots \frac{\partial}{\partial P^{\mu N}} e^{-t\Delta}, \tag{A.1}$$

where $\Delta = P^2 + M^2 - i\varepsilon$. After taking the derivatives the remaining integral is related to the Γ function, i.e.,

$$\int_0^{\infty} \mathrm{d}t\, t^{z-1} \mathrm{e}^{-t\Delta} = \Gamma(z)\Delta^{-z}. \tag{A.2}$$

INTEGRALS WITH THREE DENOMINATORS

After performing the momentum integrations there are only two integrals to be evaluated, J_1 and J_2, which are:

$$J_1(\beta, \beta_{\mathrm{H}}) = \int_0^1 \mathrm{d}x_1 \int_0^{1-x_1} \mathrm{d}x_2 \left[1 - \beta x_1(1-x_1) + (\beta - \beta_{\mathrm{H}})x_1 x_2 - i\varepsilon\right]^{-1}, \tag{A.3}$$

$$J_2(\beta, \beta_{\mathrm{H}}) = \int_0^1 \mathrm{d}x_1 \int_0^{1-x_1} \mathrm{d}x_2 x_1 x_2 / \left[1 - \beta x_1(1-x_1) + (\beta - \beta_{\mathrm{H}})x_1 x_2 - i\varepsilon\right]. \tag{A.4}$$

The parametric integrals can be done analytically and the results are:

$$J_1(\beta, \beta_{\mathrm{H}}) = -\Delta S/(\beta - \beta_{\mathrm{H}}), \tag{A.5}$$

$$J_2(\beta, \beta_{\mathrm{H}}) = \tfrac{1}{2}(\beta - \beta_{\mathrm{H}})^{-1} + (\beta - \beta_{\mathrm{H}})^{-2}\left[\Delta S - \tfrac{1}{2}\beta \Delta L\right]. \tag{A.6}$$

The functions $S(x)$ and $L(x)$ are the complex conjugate of those defined in the appendix of ref. [15]. However notice a misprint in eq. (A.4c) of this reference. To the real part of $S(\beta)$ one should add $-\frac{1}{2}\pi^2$.

INTEGRALS WITH FOUR DENOMINATORS

There are two types of integrals coming from the diagrams with four denominators, depending if it is a W or a Z that circulates in the loop. For the box with the W's we obtain

$$\begin{aligned} I_{\mathrm{W}}^{+}(\beta, \beta_{\mathrm{H}}, \theta) &= 4\int_0^1 \mathrm{d}x_1 \int_0^{1-x_1} \mathrm{d}x_2 \int_0^{1-x_1-x_2} \mathrm{d}x_3 \\ &\quad \times \left\{\left[1 - x_1 - x_2 - x_3(x_1 + x_2)\right]/\Delta_+^2 + x_2(1-x_3)/\Delta_-^2\right\}, \\ I_{\mathrm{W}}^{-}(\beta, \beta_{\mathrm{H}}, \theta) &= I_{\mathrm{W}}^{+}(\beta, \beta_{\mathrm{H}}, \theta + \pi), \end{aligned} \tag{A.8}$$

where

$$\Delta_{\pm} = 1 - x_1 - \beta x_2(1 - x_1 - x_2) + \left[\beta_{\mp} x_2 + \beta_{\pm}(x_1 + x_2)\right]x_3, \tag{A.9}$$

$$\beta_{\pm} = \tfrac{1}{2}(\beta - \beta_{\mathrm{H}})(1 \pm \cos\theta). \tag{A.10}$$

The x_3 integration can be done easily and the result is:

$$I_W^+ = 4\int_0^1 dx_1 \int_0^{1-x_1} dx_2$$

$$\times \left\{ \frac{(1-x_1-x_2)^2}{a[a+b_+(1-x_1-x_2)]} + \frac{x_2(1-x_1-x_2)}{a[a+b_-(1-x_1-x_2)]} \right.$$

$$- \frac{x_1+x_2}{b_+}\left[\frac{1}{b_+}\ln\left(1+\frac{b_+}{a}(1-x_1-x_2)\right) - \frac{1-x_1-x_2}{a+b_+(1-x_1-x_2)}\right]$$

$$\left. - \frac{x_2}{b_-}\left[\frac{1}{b_-}\ln\left(1+\frac{b_-}{a}(1-x_1-x_2)\right) - \frac{1-x_1-x_2}{a+b_-(1-x_1-x_2)}\right]\right\}, \quad \text{(A.11)}$$

where

$$a = 1 - x_1 - \beta x_2(1-x_1-x_2),$$

$$b_\pm = \beta_\mp x_2 + \beta_\pm(x_1+x_2). \quad \text{(A.12)}$$

For the box with Z's we have

$$I_Z^+ = 4\int_0^1 dx_1 \int_0^{1-x_1} dx_2 \int_0^{x_2} dx_3 x_2 x_3 \Delta_Z^{-2}, \quad \text{(A.13a)}$$

$$I_Z^- = -4\int_0^1 dx_1 \int_0^{1-x_1} dx_2 \int_0^{x_2} dx_3 x_1(1-x_2)\Delta_Z^{-2}, \quad \text{(A.13b)}$$

where

$$\Delta_Z = x_1(1+\beta_- x_2) + (1+\beta_+(1-x_2) - \beta x_1)x_3. \quad \text{(A.14)}$$

Again the x_3 integration is easy and leads to:

$$I_Z^+ = 4\int_0^1 dx_1 \int_0^{1-x_1} dx_2 \frac{x_2}{d}\left\{\frac{1}{d}\ln\left(1+\frac{d}{c}x_2\right) - \frac{x_2}{c+dx_2}\right\}, \quad \text{(A.15a)}$$

$$I_Z^- = -4\int_0^1 dx_1 \int_0^{1-x_1} dx_2 \frac{x_1 x_2(1-x_2)}{c(c+dx_2)}, \quad \text{(A.15b)}$$

where

$$c = x_1(1+\beta_- x_2),$$

$$d = 1 + \beta_+(1-x_2) - \beta x_1. \quad \text{(A.16)}$$

The x_1 and x_2 integrals can be done analytically [16]. In spite of that, in our case a trivial numerical integration turned out to be easier. Notice that for $\sqrt{s} < 2M_{W,Z}$ the denominators never vanish which means that there are no poles to be avoided.

References

[1] S.L. Glashow, Nucl. Phys. 22 (1961) 579;
S. Weinberg, Phys. Rev. Lett. 19 (1967) 1264;
A. Salam, *in* Elementary particle theory: relativistic groups and analyticity, Nobel Symp. No. 8, ed. N. Svartholm (Almqvist and Wiksell, Stockholm 1968) p. 367
[2] Hasert et al., Phys. Lett. 46B (1973) 121
[3] G. Arnison et al., Phys. Lett. 122B (1983) 103;
P. Bagnaia et al., Phys. Lett. 129B (1983) 130
[4] P.W. Higgs, Phys. Rev. Lett. 12 (1964) 132
[5] A.D. Linde, Zh. Eksp. Teor. Fiz. Pis'ma Red. 23 (1976) 73 (JETP Lett. 23 (1976) 64);
S. Weinberg, Phys. Rev. Lett. 36 (1976) 294
[6] M. Veltman, Nucl. Phys. B123 (1977) 89;
B.W. Lee, C. Quigg and H.B. Thacker, Phys. Rev. D16 (1977) 1519
[7] J.P. Leveille, Phys. Lett. 83B (1979) 123
[8] R. Bates and J.N. Ng, Phys. Rev. D32 (1985) 51
[9] J.D. Bjorken, *in* Proc. SLAC Summer Institute on particle physics, SLAC report no. 198 (1976);
P. Kalyniak, J.N. Ng and P. Zakaranskas, Phys. Rev. D29 (1984) 502
[10] R.N. Cahn, M.S. Chanowitz and N. Fleishon, Phys. Lett. 82B (1979) 113
[11] T.G. Rizzo, Ames Laboratory preprint, IS-J1652 (1985)
[12] Z.Z. Aydin, S.A. Baran and A.O. Barut, Nucl. Phys. B55 (1973) 601
[13] S. Sakakibara, Phys. Rev. D24 (1981) 1149;
S. Sakakibara, *in* Radiative corrections in SU(2) × U(1), ed. B.W. Lynn et al. (World-Scientific, Singapore, 1984)
[14] D.A. Ross and J.C. Taylor, Nucl. Phys. B51 (1973) 125; (E) B58 (1973) 643
[15] A. Barroso, F. Boudjema, J. Cole and N. Dombey, Z. Phys. C28 (1985) 149
[16] G. 't Hooft and M. Veltman, Nucl. Phys. B153 (1979) 365